Journal of Advanced Ceramics
2022, **11**(4): 582–588
https://doi.org/10.1007/s40145-021-0558-y
ISSN 2226-4108
CN 10-1154/TQ

Research Article

High transmittance and grain-orientated alumina ceramics fabricated by adding fine template particles

Han CHEN[a,c], Jin ZHAO[b,c], Shunzo SHIMAI[c], Xiaojian MAO[b,c], Jian ZHANG[b,c], Guohong ZHOU[b,c], Shiwei WANG[b,c,*], Na GU[d], Kai ZHENG[d]

[a]*University of Chinese Academy of Sciences, Beijing 100049, China*
[b]*Center of Materials Science and Optoelectronics Engineering, University of Chinese Academy of Sciences, Beijing 100049, China*
[c]*State Key Laboratory of High Performance Ceramics and Superfine Microstructure, Shanghai Institute of Ceramics, Chinese Academy of Sciences, Shanghai 200050, China*
[d]*Shandong Guiyuan Advanced Ceramics Co., Ltd., Zibo 255000, China*

Received: July 9, 2021; Revised: November 25, 2021; Accepted: November 26, 2021

Abstract: Transparent Al_2O_3 ceramics with grains aligned to the *c*-axis were prepared by adding platelets with a low aspect ratio into fine equiaxed particles. The mixed powders were formed into green bodies using spontaneous coagulation casting and sintered by pressureless sintering and hot-isostatic pressure sintering. Zeta potentials and rheological behavior of the slurries, relative densities of green bodies, and orientation and optical properties of sintered bodies were investigated and discussed. The platelet with a high aspect ratio suppressed densification more seriously during sintering than the one with a low aspect ratio. An excellent oriented structure was obtained when 5 wt% platelets with a low aspect ratio were added, and transparent Al_2O_3 ceramics with grains aligned to *c*-axis were successfully prepared; the in-line transmittance was 78.4% at 600 nm, which is the highest one in the currently reported literature.

Keywords: templated grain growth (TGG); orientation; transparent alumina

1 Introduction

Templated grain growth (TGG) is an effective technique to prepare textured ceramics [1–4], matrix particles with equiaxed structure were mixed with plate-like or rod-like template particles, and then template particles can be homogeneously distributed and oriented in the matrix by extrusion or tape casting [5,6]. Subsequent heat treatment, such as hot pressing and hot forging, would result in oriented nucleation and preferred orientation growth. Texture degree and required anisotropic properties of materials can be adjusted by sufficient template addition and appropriate heat treatment methods [7–9]. Many types of textured ceramics including α-Al_2O_3 [7,10,11], Si_3N_4 [5,8], SiC [12], BN [13], and piezoceramics [14–17] have been formed by TGG.

The fabrication of textured alumina ceramics using platelets as template was studied by Brandon *et al.* [1,2] and Suvaci *et al.* [3] in the 1990s. To date, many studies have been focused on microstructure development,

* Corresponding author.
E-mail: swwang51@mail.sic.ac.cn

mechanical strength, dielectric properties, and optical properties of textured alumina prepared by TGG method. Snel *et al*. [18] qualitatively studied the effect of different tape casting parameters using a platelet with an aspect ratio of 30, and concluded carrier tape speed, gap height, and deairing time those all could influence the grain orientation of the sintered body. Takatori *et al*. [19] studied the effect of platelet aspect ratio on orientation degree, and demonstrated the platelet with an aspect ratio of 10 produced sintered bodies with the highest texture ($f_{(006)+(1010)} \approx 0.7$–$0.8$). Seabaugh *et al*. [7] used a platelet with an aspect ratio of 6 and approximately 5% CaO and SiO_2 as sintering aids, and concluded that the sintering aid at high temperatures was effective for achieving orientation of the sintered body. Zhang *et al*. [20] used a platelet with an aspect ratio of about 10 to study the effects of orientation degree and microstructure on crack propagation behavior, fracture toughness, and strength of alumina ceramics, and concluded that grain-oriented alumina ceramics possessed higher toughness. Schlup *et al*. [21] analyzed the effect of hot-pressing parameters on the densification and optical properties of textured alumina using a platelet with an aspect ratio of 22, and found that the increase in temperature improved the optical properties at the expense of enhanced grain growth. Our previous study [22] verified the feasibility of preparing alumina transparent ceramics using a platelet with an aspect ratio of 10, and the in-line transmittance has been increased to about 60%, but a few residual pores in the grain boundaries limited the further increase in transmittance.

The above studies on TGG of textured alumina were focused on platelets with high aspect ratio, showing that a highly oriented structure could be achieved, and the densification was suppressed compared with those using only equiaxed particles, leaving residual pores in the final ceramics which were detrimental to transmittance. The present study is intended to examine the feasibility of the production of dense alumina ceramics with oriented grains by adding platelets with low aspect ratio into submicron alumina particles. The effects of the platelet (size and amount) and the sintering conditions (temperature, duration, and pressure) on the development of microstructure, orientation degree, and optical properties of ceramics were systematically investigated.

2 Materials and methods

High purity submicron alumina powder (CR-10, Baikowski, Annecy, France) containing 600 ppm MgO as sintering aid was selected as matrix powder. Two α-Al_2O_3 platelets (platelet D with an aspect ratio of 4–6, major axis of 2–3 μm, and minor axis of 0.5 μm; platelet DN with an aspect ratio of 10, major axis of 5 μm, and minor axis of 0.5 μm; their *c*-axis normal to the major facet) were selected as templates. Morphology of platelet D is shown in Fig. 1. Copolymers of isobutylene and maleic anhydride with molecular weights of 5500–6500 (Isobam 600AF, Kuraray, Japan) and 55,000–65,000 (Isobam 104, Kuraray, Japan) [23,24] were used as dispersing and coagulation agents for alumina slurry, respectively.

Alumina slurries were prepared as follows: Firstly, Isobam agents were dissolved in deionized water. Secondly, α-Al_2O_3 platelets were added in the Isobam solution and mechanically stirred for 2–3 min. Thirdly, CR-10 alumina powder was added and ball milled in a planetary mill for 1 h. Solid loading of the slurries were 40 vol%, and the addition of platelets was 1–5 wt%. The addition of Isobam 600AF and Isobam 104 were 0.3 and 0.2 wt% (relative to the weight of alumina), respectively. After milling, the slurry was degassed and cast into a plastic mold, and the shearing force generating in flow was used to align the platelets [22]. After coagulation and drying, green bodies were pre-sintered at 800 ℃ for 2 h in air to burn out the organic additives. Final sintering was conducted by pressureless sintering or hot isostatic press (HIP) sintering, pressureless sintering was carried out at 1860 ℃ for 12 h in vacuum, and HIP sintering was carried out at 1850 ℃ for 3 h in argon with 200 MPa (samples for HIP were pre-sintered at 1840 ℃ for 6 h in vacuum).

Zeta potentials of dilute alumina slurries (diluted from 40 vol% solid loading slurry to the ratio of alumina/

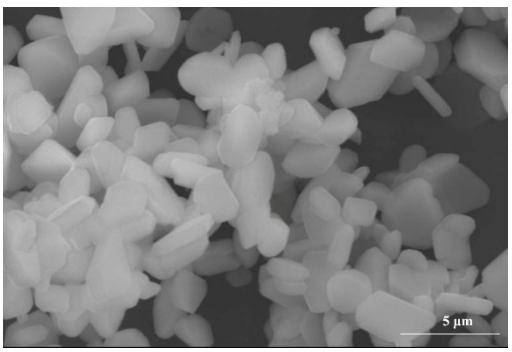

Fig. 1 Morphology of α-Al_2O_3 platelet D.

water as 0.2 g/L) were measured using the electrophoretic mobility (Zeta Plus, Bruker Inc., Holtsville, USA). The rheological behavior of the slurries was characterized via a rotational rheometer (HAAKE Viscotester iQ Air, Thermo Fisher Scientific, USA) with a parallel plate (20 mm in diameter). Microstructures of the green bodies and sintered ceramics were observed using a scanning electron microscope (JSM-6390LV, JEOL, Tokyo, Japan). Linear intercept analysis based on the equation $GS = 1.56L$ (L: average intercept) was used for measuring the average grain size. The relative density of the ceramics was measured by Archimedes method in distilled water. The evolution of X-ray diffraction (XRD) peaks was characterized on the top surfaces of the ceramic in the 2θ range from 10° to 90° with a step of 0.05° by an X-ray diffractometer (D8 Advance, Bruker Inc., Germany) with Cu Kα radiation. The degree of orientation (f value) for each specimen was evaluated according to the Lotgering method [25] from the XRD diffraction peaks. Ceramics were ground and double-surface polished to 1 mm thick to test in-line transmittance using a spectrophotometer (V-770, JASCO, Tokyo, Japan), and the angle of scattered light was 0.5°.

3 Results and discussion

3.1 Zeta potentials of the dilute alumina slurries

Zeta potentials of dilute alumina slurries (powder/water: 0.2 g/L) are shown in Fig. 2. It is observed that the isoelectric point was about pH = 2.8 for the slurry containing platelet D (black line) and was about pH = 3 for the slurry containing platelet DN (pink line), lower than that of the slurry containing equiaxed alumina particles only, which has an isoelectric point of pH ≈ 8–10 [26]. The difference between the isoelectric point of platelets and equiaxed alumina particles can be explained by the different types of surface hydroxyl groups [27,28]. The surface structure of the basal planes of platelets is comprised primarily of doubly coordinated surface hydroxyl groups, and that of the equiaxed alumina particle is composed primarily of singly coordinated surface hydroxyl groups. The isoelectric point of the slurry moved to the left (pH ≈ 2) when the dispersant was added. At the same time, the absolute value of the zeta potential of slurry changed from 12.4 to 33.8 mV when the pH of the slurry was in the neutral range (pH ≈ 7). That means the dispersant can be adsorbed on the platelets and disperse the platelets. The blue line shows the zeta potential of the diluted slurry prepared by adding 5 wt% platelet D and 95 wt% equiaxed alumina powder, the isoelectric point of the slurry was 2.3, and the absolute value of the zeta potential of the slurry was about 21.2 mV (in the neutral range of pH ≈ 7), which ensures the preparation of slurries with high solid loading and low viscosity.

3.2 Rheological behavior of slurries

The viscosity of the slurries is shown in Fig. 3. The viscosity was decreased a bit with the increase of platelet addition. For example, the viscosity was ~0.25 Pa·s at 100 s^{-1} for the slurry containing 1 wt% platelet D, and 0.23 Pa·s at 100 s^{-1} for the slurry containing 5 wt% platelet D. The viscosity of the slurry containing platelet DN was lower than that with platelet D, e.g., 0.22 Pa·s at 100 s^{-1} for the slurry containing 1 wt% platelet DN. The platelet DN has a higher absolute value of zeta potential in the neutral range, which benefited particle dispersion. Low viscosity benefits slurry flowability, which has a positive effect on

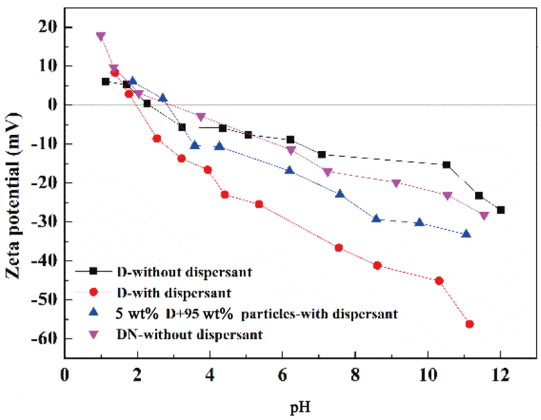

Fig. 2 Zeta potentials of dilute alumina slurries.

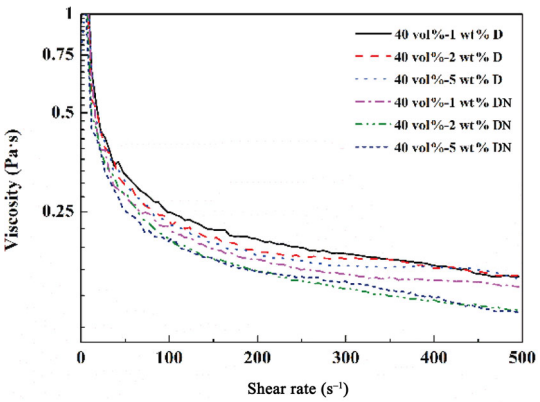

Fig. 3 Viscosity of the slurries containing different amount of platelets.

the alignment of platelet and is helpful for the preparation of grain-oriented ceramics [29].

3. 3 Densities of green bodies and sintered bodies

Table 1 shows the densities of green bodies containing different amount of platelets. The relative densities of green bodies containing platelet D were higher than those containing platelet DN, e.g., 48.2% for the green body containing 1 wt% platelet D and 48.0% for the green body containing 1 wt% platelet DN, which means platelets with low aspect ratio are useful for the increase of particle packing density. The relative density of green body decreased with the increase of platelet addition, e.g., 48.2% for the green body containing 1 wt% platelet D and 47.6% for the green body containing 5 wt% platelet D. That is because equiaxed particles are easier to pack a higher density green body compared to platelets.

Figure 4 shows the effects of sintering temperature on relative densities of sintered bodies containing different amount of platelets. Take the green body containing 1 wt% platelet D for example, the relative density was increased to 61.2% at 1200 ℃ and that means densification began. The relative densities were fast increased to 85.9% and 98.5% when the sintering temperatures were 1300 and 1400 ℃, respectively. The relative density (67.8%) of the sample with 5 wt% platelet D was higher than that (61.2%) of the sample with 1 wt% platelet D and that (61.9%) of the sample without platelet D when the sintering temperature was 1200 ℃. The possible reason is that more platelets may provide more power to "absorb" or "swallow" fine particles and benefit densification during the initial growth process. When the temperature was increased to 1400 ℃, the relative density of the sample containing 5 wt% platelet D was 95.9%, lower than that of the sample with 1 wt% platelet D (98.5%). It confirmed that the addition of more platelets was harmful for densification. Anyway, during the whole sintering process, relative densities of green bodies containing platelet D were higher than those containing platelet DN, e.g., 95.9% for the green body containing 5 wt% platelet D and 95.3% for the green body containing 5 wt% platelet DN at 1400 ℃, which indicates that the addition of low aspect ratio platelets is easier for densification.

Table 1 Relative densities of green bodies

Sample	Without platelet	Adding platelet D			Adding platelet DN		
		1 wt%	2 wt%	5 wt%	1 wt%	2 wt%	5 wt%
Relative density (%)	49.2	48.2	47.8	47.6	48.0	47.7	47.4

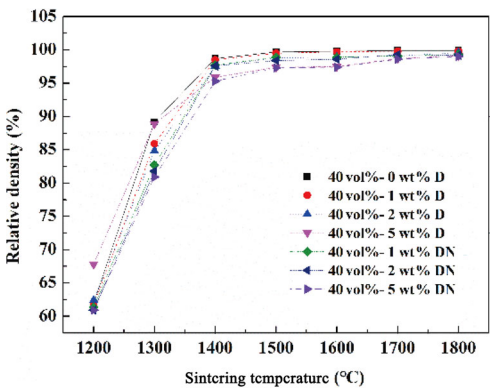

Fig. 4 Effect of temperature on relative densities of the green bodies containing different amount of platelets.

3. 4 Effect of platelet addition on orientation

Figure 5 shows the XRD patterns of sintered bodies with different amount of platelets, and the pressureless sintering parameter was 1860 ℃ for 12 h in vacuum. It can be seen from Fig. 5 that the intensity of (006) crystal plane of ceramics with 1 wt% platelet D has not been obviously enhanced. For the sample with 2 wt% platelet D, the intensity of (006) crystal plane became the strongest one, and the orientation degree of ceramics was about 51.9%, which means the sample was obviously textured. When the platelet addition was increased to 5 wt%, only one diffraction peak corresponding to (006) was found in the XRD pattern, and the orientation degree of ceramics was close to 100%, which means the perfect oriented structure was formed. Although the ceramic by adding 1 wt% platelet with low aspect ratio was difficult to be textured, an excellent oriented

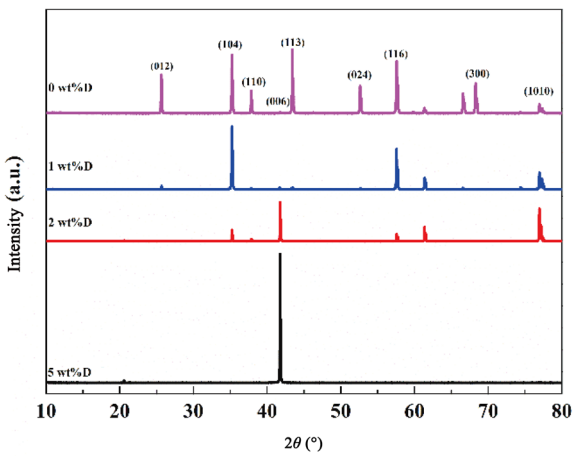

Fig. 5 XRD patterns of sintered bodies with different amount of platelets.

structure can be obtained when the proper addition amount of the platelet and sintering conditions were employed.

3. 5 Effect of platelet addition on in-line transmittance

Figure 6 shows the in-line transmittance of samples with different amount of platelets and pressureless sintered at 1860 ℃ for 12 h in vacuum. The sample without platelet D showed an in-line transmittance of 29% at 600 nm, and the samples with 1 and 2 wt% platelet D had an in-line transmittance of 31.4% and 57.3% at 600 nm, respectively. However, the sample with 5 wt% platelets showed the lowest in-line transmittance, 26.7% at 600 nm, even lower than the sample without platelet D.

In order to figure out the reason for the lowest in-line transmittance of the sample with 5 wt% platelets, SEM microphotographs of acid-etched fracture surfaces after ground and polished were taken, and the results are shown in Fig. 7. The grain sizes of samples increased from 69.1 to 73.0 and 82.9 μm when the addition of platelets was increased from 1 to 2 and 5 wt% platelets, respectively. Noticeable non-uniform grains along with residual pores were found in all samples, especially in the sample with 5 wt% platelets. As we know, samples with a large amount of platelets are difficult to be densified, and this explains why the sample with 5 wt% platelets had a low in-line transmittance though it had a high orientation degree (Fig. 5). With all this in mind, it can be summarized that the introduction of a large amount of platelets results in higher crystallographic texture, and it adversely affects the densification and results in residual pores in ceramics. The pores negate the improvement in optical properties.

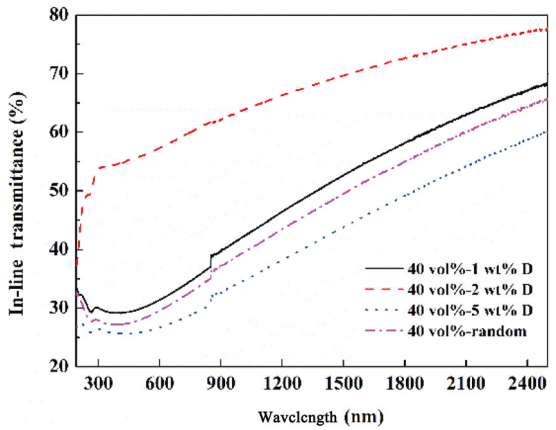

Fig. 6 In-line transmittance of samples with different amount of platelets pressureless sintered at 1860 ℃ for 12 h.

HIP sintering is an effective method to increase the density [30]. Here, HIP sintering was employed to enhance the densification of the samples with platelets. Green bodies were pressureless pre-sintered at 1840 ℃ for 6 h in vacuum, and then HIP sintering was carried out at 1850 ℃ for 3 h in argon with 200 MPa. In-line transmittance of the pressureless pre-sintered and HIPed samples with different amount of platelets is shown in Fig. 8. The sample with 1 wt% platelets showed higher transmittance compared with that sintered without HIP (Fig. 6), but the improvement is not so obvious because of its random structure (Fig. 5). The sample with 2 wt% platelets showed higher transmittance (54.4% at 600 nm) than that sintered without HIP (Fig. 6), and this improvement is obvious on account of its texture structure. The sample with 5 wt% platelets shows the highest in-line transmittance, 78.4% at 600 nm (Fig. 8). To the extent of the authors' knowledge, this is the highest in-line transmission reported in the literature for polycrystalline alumina till now [21,31–35]. The photograph of the sample is inserted in Fig. 8, and the printed letters behind the ceramic can be clearly seen. This result demonstrated the feasibility of the production of dense alumina ceramics with uniaxially oriented grains by adding low aspect ratio platelets in submicron alumina particles, and the optical property was significantly improved due to crystallographic orientation and further HIP sintering. With the help of high pressure, ceramics

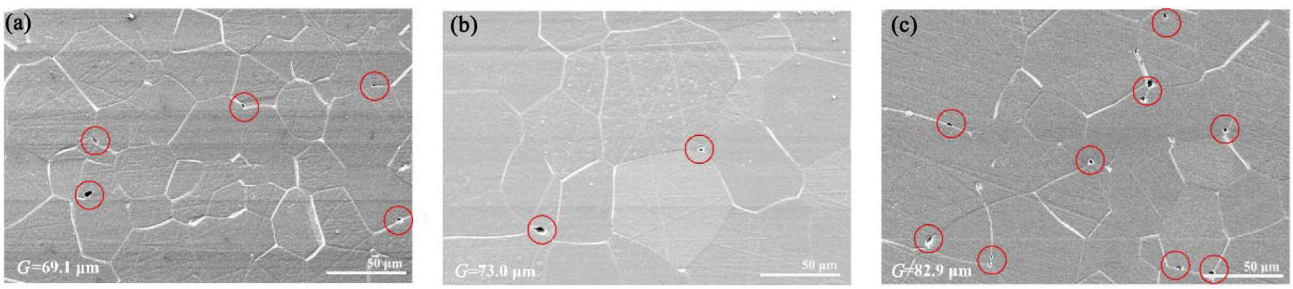

Fig. 7 SEM microphotographs of acid-etched surfaces of ceramics containing (a) 1 wt%, (b) 2 wt%, and (c) 5 wt% platelet D, pressureless sintered at 1860 ℃ for 12 h.

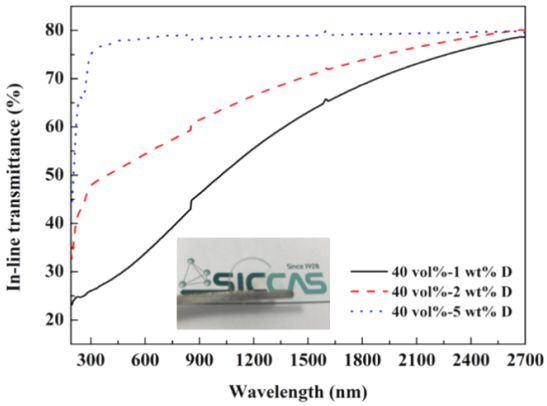

Fig. 8 In-line transmittance of samples with different amount of platelets, which were pressureless pre-sintered at 1840 ℃ for 6 h and HIPed at 1850 ℃ for 3 h in argon with 200 MPa. Inset: the photograph of alumina ceramic containing 5 wt% platelet D.

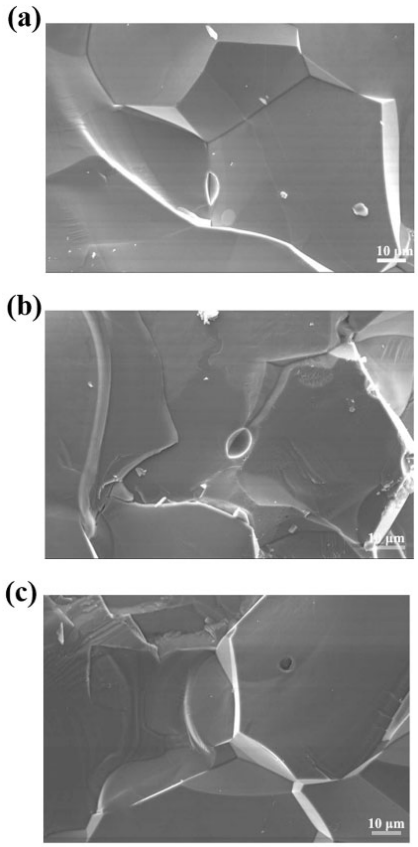

Fig. 9 Fracture surfaces of ceramics containing (a) 1 wt%, (b) 2 wt%, and (c) 5 wt% platelet D, pressureless pre-sintered at 1840 ℃ for 6 h and HIPed at 1850 ℃ for 3 h in argon with 200 MPa.

became denser, and the residual pores (Fig. 9) were less than those sintered without HIP (Fig. 7). However, the in-line transmittance of the present ceramics still has a gap with the theoretical one (86%) of sapphire because there were still some residual pores in the grain boundaries or grains. The processing parameters including the particle packing state in the green body and pre-sintering conditions, and HIP conditions need to be further optimized in the near future.

4 Conclusions

Dense alumina ceramics with oriented grains were prepared by the template grain growth. The densification rate of the ceramics adding platelets with low aspect ratio was faster than that with a high aspect ratio. The density of the ceramics increased with the temperature and decreased with the addition of platelets. The orientation degree of ceramics increased with the addition of platelets, and an excellent oriented structure was obtained when 5 wt% platelets with low aspect ratio were added. Transparent α-Al_2O_3 ceramics with grains aligned to the *c*-axis were successfully prepared by pre-sintering and hot-isostatic pressure sintering, and the in-line transmittance was 78.4% at 600 nm (1 mm thick), which is the highest value currently reported.

Acknowledgements

This work was supported by the National Natural Science Foundation of China (Nos. 51772309 and 52130207). The authors thank Prof. Jing WANG (Dalian University of Technology) for the synthesis of Al_2O_3 platelets.

References

[1] Brandon D, Chen DZ, Chan H. Control of texture in monolithic alumina. *Mater Sci Eng A* 1995, **195**: 189–196.

[2] Carisey T, Leviri I, Brandon DG. Micro structure and mechanical properties of textured Al_2O_3. *J Eur Ceram Soc* 1995, **15**: 283–289.

[3] Suvaci E, Seabaugh MM, Messing GL. Reaction-based processing of textured alumina by templated grain growth. *J Eur Ceram Soc* 1999, **19**: 2465–2474.

[4] Zhang Z, Duan XM, Qiu BF, *et al*. Preparation and anisotropic properties of textured structural ceramics: A review. *J Adv Ceram* 2019, **8**: 289–332.

[5] Zhu XW, Sakka Y. Textured silicon nitride: Processing and anisotropic properties. *Sci Technol Adv Mater* 2008, **9**: 033001.

[6] Walton RL, Vaudin MD, Hofer AK, *et al*. Tailoring particle alignment and grain orientation during tape casting and templated grain growth. *J Am Ceram Soc* 2019, **102**: 2405–2414.

[7] Seabaugh MM, Messing GL, Vaudin MD. Texture development and microstructure evolution in liquid-phase-

sintered α-alumina ceramics prepared by templated grain growth. *J Am Ceram Soc* 2000, **83**: 3109–3116.

[8] Jiang QG, Liu J, Guo WM, *et al*. A novel hot pressing flowing sintering for preparation of texturing ceramics. *J Am Ceram Soc* 2015, **98**: 2696–2699.

[9] Pavlacka RJ, Messing GL. Processing and mechanical response of highly textured Al_2O_3. *J Eur Ceram Soc* 2010, **30**: 2917–2925.

[10] Seabaugh MM, Vaudin MD, Cline JP, *et al*. Comparison of texture analysis techniques for highly oriented α-Al_2O_3. *J Am Ceram Soc* 2000, **83**: 2049–2054.

[11] Seabaugh MM, Kerscht IH, Messing GL. Texture development by templated grain growth in liquid-phase-sintered α-alumina. *J Am Ceram Soc* 1997, **80**: 1181–1188.

[12] Sacks MD, Scheiffele GW, Staab GA. Fabrication of textured silicon carbide via seeded anisotropic grain growth. *J Am Ceram Soc* 1996, **79**: 1611–1616.

[13] Xue JX, Liu JX, Xie BH, *et al*. Pressure-induced preferential grain growth, texture development and anisotropic properties of hot pressed hexagonal boron nitride ceramics. *Scripta Mater* 2011, **65**: 966–969.

[14] Kwon S, Sabolsky EM, Messing GL, *et al*. High strain, <001> textured $0.675Pb(Mg_{1/3}Nb_{2/3})O_3$–$0.325PbTiO_3$ ceramics: Templated grain growth and piezoelectric properties. *J Am Ceram Soc* 2005, **88**: 312–317.

[15] Maurya D, Pramanick A, An K, *et al*. Enhanced piezoelectricity and nature of electric-field induced structural phase transformation in textured lead-free piezoelectric $Na_{0.5}Bi_{0.5}TiO_3$–$BaTiO_3$ ceramics. *Appl Phys Lett* 2012, **100**: 172906.

[16] Li P, Zhai JW, Shen B, *et al*. Ultrahigh piezoelectric properties in textured (K,Na)NbO_3-based lead-free ceramics. *Adv Mater* 2018, **30**: 1705171.

[17] Chang YF, Sun Y, Wu J, *et al*. Formation mechanism of highly $[001]_c$ textured $Pb(In_{1/2}Nb_{1/2})O_3$–$Pb(Mg_{1/3}Nb_{2/3})O_3$–$PbTiO_3$ relaxor ferroelectric ceramics with giant piezoelectricity. *J Eur Ceram Soc* 2016, **36**: 1973–1981.

[18] Snel MD, van Hoolst J, de Wilde AM, *et al*. Influence of tape cast parameters on texture formation in alumina by templated grain growth. *J Eur Ceram Soc* 2009, **29**: 2757–2763.

[19] Takatori K, Kadoura H, Matsuo H, *et al*. Microstructural evolution of high purity alumina ceramics prepared by a templated grain growth method. *J Ceram Soc Jpn* 2016, **124**: 432–441.

[20] Zhang MM, Chang YF, Bermejo R, *et al*. Improved fracture behavior and mechanical properties of alumina textured ceramics. *Mater Lett* 2018, **221**: 252–255.

[21] Schlup AP, Costakis Jr WJ, Rheinheimer W, *et al*. Hot-pressing platelet alumina to transparency. *J Am Ceram Soc* 2020, **103**: 2587–2601.

[22] Chen H, Shimai S, Zhao J, *et al*. Highly oriented α-Al_2O_3 transparent ceramics shaped by shear force. *J Eur Ceram Soc* 2021, **41**: 3838–3843.

[23] Sun Y, Shimai S, Peng X, *et al*. A method for gelcasting high-strength alumina ceramics with low shrinkage. *J Mater Res* 2014, **29**: 247–251.

[24] Yang Y, Shimai S, Wang SW. Room-temperature gelcasting of alumina with a water-soluble copolymer. *J Mater Res* 2013, **28**: 1512–1516.

[25] Lotgering FK. Topotactical reactions with ferrimagnetic oxides having hexagonal crystal structures—I. *J Inorg Nucl Chem* 1959, **9**: 113–123.

[26] Hashiba M, Okamoto H, Nurishi Y, *et al*. The zeta-potential measurement for concentrated aqueous suspension by improved electrophoretic mass transport apparatus—Application to Al_2O_3, ZrO_3 and SiC suspensions. *J Mater Sci* 1988, **23**: 2893–2896.

[27] Franks GV, Gan Y. Charging behavior at the alumina–water interface and implications for ceramic processing. *J Am Ceram Soc* 2007, **90**: 3373–3388.

[28] Tsyganenko AA, Mardilovich PP. Structure of alumina surfaces. *Faraday Trans* 1996, **92**: 4843.

[29] Suzuki TS, Uchikoshi T, Sakka Y. Control of texture in alumina by colloidal processing in a strong magnetic field. *Sci Technol Adv Mater* 2006, **7**: 356–364.

[30] She JH, Guo JK, Jiang DL. Hot isostatic pressing of α-silicon carbide ceramics. *Ceram Int* 1993, **19**: 347–351.

[31] Mao XJ, Wang SW, Shimai S, *et al*. Transparent polycrystalline alumina ceramics with orientated optical axes. *J Am Ceram Soc* 2008, **91**: 3431–3433.

[32] Yi HL, Mao XJ, Zhou GH, *et al*. Crystal plane evolution of grain oriented alumina ceramics with high transparency. *Ceram Int* 2012, **38**: 5557–5561.

[33] Costakis Jr WJ, Schlup A, Youngblood JP, *et al*. Aligning α-alumina platelets via uniaxial pressing of ceramic-filled polymer blends for improved sintered transparency. *J Am Ceram Soc* 2020, **103**: 3500–3512.

[34] Krell A, Blank P, Ma HW, *et al*. Transparent sintered corundum with high hardness and strength. *J Am Ceram Soc* 2003, **86**: 12–18.

[35] Pringuet A, Takahashi T, Baba S, *et al*. Fabrication of transparent grain-oriented polycrystalline alumina by colloidal processing. *J Am Ceram Soc* 2016, **99**: 3217–3219.